Analysis of the Improvement in Implied Meridional Ocean Energy Transport as Simulated by the NCAR CCM3*

JAMES J. HACK

National Center for Atmospheric Research,+ Boulder, Colorado

(Manuscript received 1 July 1997, in final form 13 November 1997)

ABSTRACT

The implied meridional ocean energy transport diagnosed from uncoupled integrations of two atmospheric general circulation models—the National Center for Atmospheric Research Community Climate Model versions 2 and 3 (CCM2 and CCM3)—shows radically different transport characteristics throughout much of the Southern Hemisphere. The CCM2 simulation requires an equatorward transport of energy by the oceans, and the CCM3 exhibits a poleward energy transport requirement, very similar to what is derived from observational analyses. Previous studies have suggested that errors in the implied ocean energy transport are largely attributable to errors in the simulated cloud radiative forcing. The results of this analysis show that although the proper simulation of the radiative effects of clouds is likely to be a necessary condition for realistic meridional ocean energy transport, it is not sufficient. Important changes in the CCM3 equatorial surface latent heat fluxes, associated with a deep formulation for parameterized moist convection, are primarily responsible for the improved ocean energy transport, where this change in the surface energy budget is much more weakly reflected in top-of-atmosphere differences in cloud radiative forcing.

1. Introduction

In the long-term mean the net solar energy absorbed by the earth's climate system must be balanced by infrared energy radiated to space. The meridional distribution of these two quantities leads to a radiative energy excess in the Tropics and a radiative energy deficit in the polar regions. The required meridional transport of energy from the equator to the poles is achieved by both the atmospheric and oceanic general circulation, where observational estimates, indicate that atmospheric transport processes dominate, particularly poleward of 30° (e.g., Carissimo et al. 1985; Savijärivi 1988; Trenberth and Solomon 1994). Nevertheless, the ocean component is a significant fraction of the overall meridional energy transport, and its proper partition in coupled atmosphere–ocean general circulation models (GCMs) is likely to be critical to the realism of any numerical simulation.

Most global atmospheric modeling work is conducted using an ''uncoupled'' framework. In this type of framework, the sea surface temperature (SST) and sea-ice distributions are prescribed in some way, thus providing strong constraints on the resulting simulation (e.g., the ocean surface properties remain perfect, regardless of any errors in the simulated surface energy budget). Despite such constraints, a number of analyses have concluded that the simulated *atmospheric* meridional heat transports in such model configurations include major errors, where these errors may be linked to uncertainties in the subgrid-scale physics (e.g., Covey 1988; Stone and Risbey 1990). A more recent analysis of the implied *ocean* energy transport (i.e., the energy transport required of the ocean circulation) in 15 uncoupled atmospheric GCMs (AGCMs) also showed significant errors among the different models, concluding that these errors were largely attributable to errors in the simulated cloud radiative forcing (Gleckler et al. 1995). In either case, inaccuracies in how the total meridional energy transport is partitioned between atmosphere and ocean is a likely source of climate drift when the two component models are coupled in an unconstrained manner. Thus, a better understanding of the source of such errors would have important scientific value.

In this paper we analyze the implied meridional ocean energy transport as diagnosed from uncoupled integrations using two versions of the National Center for Atmospheric Research (NCAR) Community Climate Model, CCM2 (Hack et al. 1993) and CCM3 (Kiehl et al. 1996). As we will show, the CCM2 simulation requires an equatorward transport of energy by the oceans over

* An electronic supplement to this article may be found on the CD-ROM accompanying this issue or at http://www.ametsoc.org/AMS.

+ The National Center for Atmospheric Research is sponsored by the National Science Foundation.

Corresponding author address: Dr. James J. Hack, NCAR/CGD, P.O. Box 3000, Boulder, CO 80307-3000.
E-mail: jhack@ucar.edu

most of the Southern Hemisphere, whereas the CCM3 simulation requires a poleward transport of energy, which is very similar to observational estimates in both magnitude and structure. Although Gleckler et al. (1995) have suggested that errors in the implied ocean energy transport are mostly linked to errors in the simulated cloud radiative forcing, we will show that details in the treatment of subgrid-scale parameterizations, in this case deep convection, are of comparable or greater importance. Numerical experiments are conducted to better understand the nature of the response. These experiments show that the radiative effects of high tropical cloud are clearly associated with improvements to the meridional energy transport by the ocean circulation, but that they do not necessarily play the dominant role.

2. Cloud radiative forcing and meridional ocean energy transport

Many aspects of the NCAR CCM2 simulation are considerably more realistic when compared with predecessor models as shown in a number of studies (e.g., Hack et al. 1994; Kiehl et al. 1994; Hurrell et al. 1993). However, a handful of important simulation errors would create serious problems for coupled modeling applications. Among these errors is that uncoupled integrations of the CCM2, using specified SSTs, produce a meridional ocean energy transport requirement that is in the wrong direction in the Southern Hemisphere when compared with observational estimates (Kiehl et al. 1998b).

Direct estimates of the ocean energy transport are very difficult to make due to inadequate three-dimensional observational data on the ocean circulation. Consequently, the ocean energy transport is often evaluated indirectly, by calculating the meridional ocean energy transport implied by the time-averaged surface energy budget. This quantity can be determined by latitudinally integrating the annually and zonally averaged net surface energy budget:

$$T_{\mathrm{O}}(\phi) = 2\pi a^2 \int_{-\pi/2}^{\phi} (S_{\mathrm{sfc}} - L_{\mathrm{sfc}} - \mathrm{LH} - \mathrm{SH}) \cos\phi' \, d\phi', \quad (1)$$

where T_{O} is the implied northward meridional energy transport at the surface, ϕ is latitude, a is the radius of the earth, S_{sfc} is the absorbed solar flux at the surface, L_{sfc} is the net longwave radiative flux at the surface, and LH and SH are the surface latent and sensible heat fluxes. Similarly, the total meridional energy transport requirement can be evaluated by integrating the net radiative energy budget at the top of the atmosphere:

$$T_{\mathrm{A+O}}(\phi) = 2\pi a^2 \int_{-\pi/2}^{\phi} (S_{\mathrm{TOA}} - L_{\mathrm{TOA}}) \cos\phi' \, d\phi', \quad (2)$$

where $T_{\mathrm{A+O}}$ is the northward meridional energy transport for the atmosphere–ocean system, and S_{TOA} and L_{TOA} are the absorbed solar flux and net longwave radiative flux at the top of atmosphere (TOA). Although the atmospheric component of the transport can be directly evaluated from atmospheric circulation statistics involving temperature, geopotential, moisture, and winds (e.g., Oort 1983), it can also be trivially determined as the residual of Eqs. (2) and (1).

The sign convention in Eqs. (1) and (2) is such that both S_{sfc} and S_{TOA} represent the respective sources of energy to the ocean and ocean–atmosphere system, and the remaining components represent energy sinks. Although this approach to evaluating meridional energy transport is generally more reliable than direct methods, there are still large uncertainties in observational estimates of the various energy terms in Eqs. (1) and (2), particularly for the surface energy components (e.g., Gleckler and Weare 1997). These observational uncertainties limit the accuracy to which the meridional energy transports can be established for both the atmosphere and ocean (e.g., Kieth 1995; Trenberth 1997). Sampling errors are generally less of a consideration for global atmospheric modeling, so meridional energy transport can be very accurately evaluated. However, we do note that the procedure we have outlined makes physical sense only if the meridional integrals (i.e., the meridional transports) go to zero at the poles. This can happen only if the simulated global energy budget is balanced. For purposes of analysis, nonzero energy imbalances can be removed with a constant correction (i.e., uniformally over the globe), where the magnitude of such corrections will be noted for all of the following results.

One of the principal highlights of the NCAR CCM3 simulation, when compared with the CCM2 simulation, is the rather dramatic improvement in the Southern Hemisphere implied ocean energy transport. This aspect of the uncoupled simulation is credited as one of the reasons for the successful NCAR Climate System Model simulations, which have demonstrated drift-free solutions without the need for artificial heat flux corrections (Boville and Gent 1998). Figure 1 shows the meridional distribution of T_{O} from CCM2 and CCM3 simulations forced with an observed SST distribution for the 5-yr period 1985–89. Energy corrections applied to the CCM2 and CCM3 T_{O} integrals were $+5.03$ W m^{-2} and -0.085 W m^{-2}, respectively. An observational estimate of T_{O} from Trenberth and Solomon (1994), which is generally representative of other studies, is also included for reference. The CCM2 shows equatorward energy transport throughout most of the Southern Hemisphere, in sharp contrast with observational estimates of this quantity. The CCM3 simulation exhibits a poleward energy transport requirement by the Southern Hemisphere oceans, very similar to the structure derived from observations, with a peak amplitude around -1×10^{15} W near 15°S. Recent work suggests that this peak value is actually within observational uncertainty, where a new

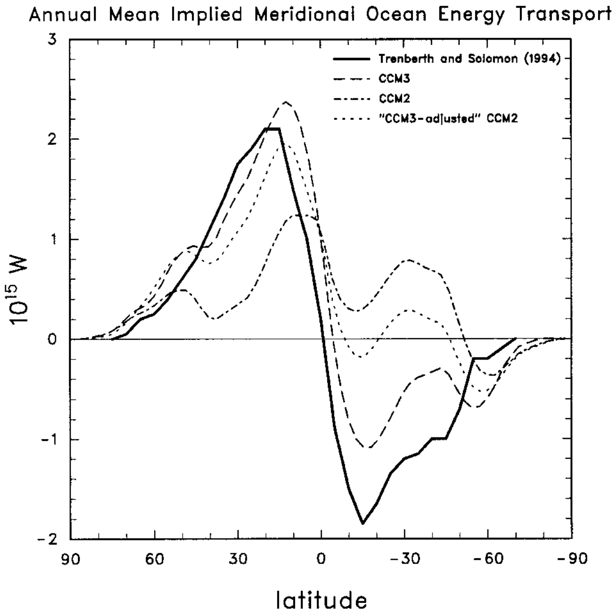

FIG. 1. Annual mean implied meridional ocean energy transport, T_O, for the CCM2, CCM3, ''CCM3-adjusted'' CCM2, and the observational estimate of Trenberth and Solomon (1994).

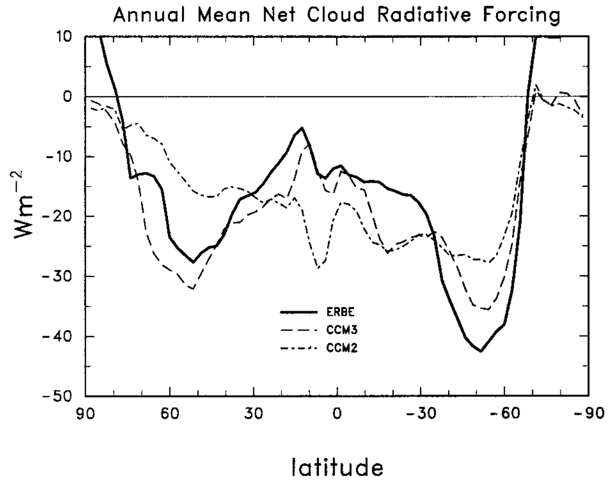

FIG. 2. Annual mean net cloud radiative forcing for the CCM2, CCM3, and ERBE.

analysis estimates peak Southern Hemisphere meridional ocean energy transport to be somewhere between -1.5×10^{15} W and -0.8×10^{15} W near 12°S (Trenberth 1997).

Earlier work by Gleckler et al. (1995) suggested that the proper representation of the TOA net cloud radiative forcing is key to a realistic implied meridional ocean energy transport. The net cloud radiative forcing (CRF) is defined as the difference between the all-sky and clear-sky net radiation (e.g., Ramanathan et al. 1989). The annual mean net cloud radiative forcing for CCM2, CCM3, and for the observational estimates derived from the Earth Radiation Budget Experiment (ERBE) (e.g., Barkstrom et al. 1990) is illustrated in Fig. 2. Indeed, this figure shows that the CCM3 simulation is in substantially better agreement with ERBE in both the Tropics and middle latitudes, largely the result of changes made to the representation of cloud radiative properties. Other measures of the TOA energy budget, along with a discussion of the reasons for the various improvements, can be found in Kiehl et al. (1998a). Based on the Gleckler et al. (1995) study, the marked improvement in the CCM3's implied meridional ocean energy transport characteristics was initially believed to be a consequence of the more realistic CCM3 TOA simulation. This assumption was examined by Hack (1997) in an analysis of the major cloud optical property modifications incorporated in the CCM3. A conclusion of this study was that the improvements in the TOA radiative energy budget only marginally altered the characteristics of the implied ocean energy transport in the Southern Hemisphere, suggesting that deficiencies in the simulated net cloud radiative forcing did not adequately account for the surface energy problems exhibited by the CCM2. Subsequent tests, in which selected CCM2 cloud optical property parameterizations were incorporated in the CCM3, confirmed that the cloud radiative forcing improvements could not explain the CCM3's radically different ocean energy transport requirements.

One way to further illustrate this finding is to adjust the CCM2 implied ocean energy transport using the CCM3 TOA radiative energy budget. The approach we utilize assumes the meridional energy transport by the atmosphere remains unchanged, allowing evaluation of how the ocean transport might change with a different TOA energy distribution. The ''adjusted'' ocean energy transport is evaluated as a residual of the new TOA and old atmospheric transports. In this case, the CCM2 atmospheric meridional energy transport can be calculated by evaluating and differencing the surface and TOA meridional energy transport integrals [Eqs. (1) and (2)]. The resulting atmospheric energy transport can then be differenced with the CCM3 TOA energy transport [evaluated using Eq. (2)] to yield an ''adjusted'' ocean meridional energy transport for the CCM2. In practice, this is the same procedure employed by Gleckler et al. (1995) to examine the role of cloud radiative forcing on ocean energy transport in a variety of AGCMs. Because of large high-latitude observational uncertainties in CRF, they used ERBE absorbed solar and outgoing longwave fluxes to construct an idealized TOA energy budget that was used to adjust ocean energy transports in each of the global models (where their CRF conclusions were reached by assuming that clear-sky effects on T_O were negligible).

The result of this type of adjustment to the CCM2 implied meridional ocean energy transport is shown by the dotted line in Fig. 1. As expected, the characteristics of the Southern Hemisphere transport are improved as a result of using the CCM3 TOA energy distribution,

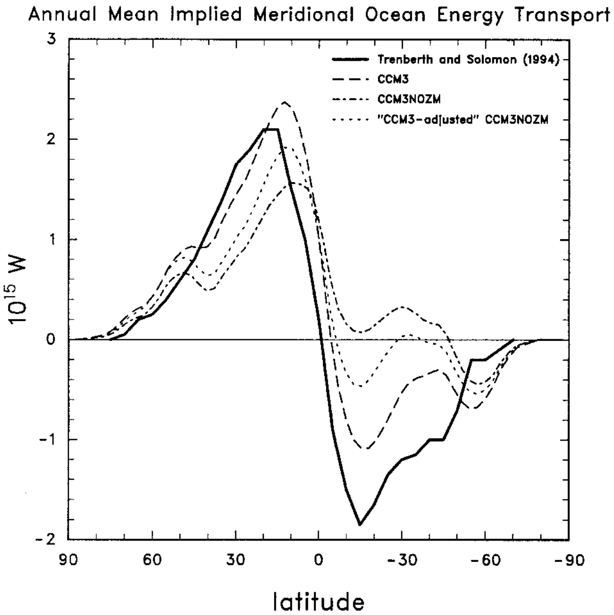

FIG. 3. Annual mean implied meridional ocean energy transport, T_O, for the CCM3NOZM experiment, CCM3, ''CCM3-adjusted'' CCM3NOZM, and the observational estimate of Trenberth and Solomon (1994).

although the improvement does not sufficiently account for the observed differences between the CCM2 and CCM3.

Consequently, the remaining physical parameterization modifications were systematically eliminated as a source of the change in ocean meridional energy transport by replacing the new CCM3 parameterization schemes with their respective CCM2 versions. This process of elimination clearly identified the introduction of the deep convection parameterization of Zhang and McFarlane (1995) as the primary source of the implied ocean energy transport change. Figure 3 shows the meridional distribution of T_O from a CCM3 simulation for which the Zhang and McFarlane (ZM) deep convection scheme has been removed (CCM3NOZM), along with the comparable CCM3 simulation results and the Trenberth and Solomon (1994) observational estimate (both as shown in Fig. 1). In the CCM3NOZM experiment, moist convection is uniquely represented using the CCM2 convection parameterization (Hack 1994), which is otherwise used in conjunction with the ZM scheme to treat shallow and midlevel convection in the CCM3. The energy correction applied to the CCM3NOZM T_O integral was -1.39 W m^{-2}. Note the strong similarity between the ''CCM3-adjusted'' CCM2 (dotted line in Fig. 1) and CCM3NOZM (dash–dotted line in Fig. 3) T_O curves. Both simulations show weak meridional transport requirements in the Southern Hemisphere, with enhanced poleward transport in the Northern Hemisphere (when compared to CCM2). This similarity suggest that, apart from the deep convection scheme, the collection of physics improvements included in the CCM3 introduce relatively minor changes to the implied ocean energy transport. The similarity also confirms the earlier result showing that the improvement in the TOA radiation budget appears to play a secondary role in the improved T_O for the CCM3 simulation; that is, the direct effects of the deep convection scheme on the surface energy budget appear to be of primary importance.

A comparison of the annual mean net cloud radiative forcing for the CCM3 and CCM3NOZM simulations indicates a sizeable change over the deep Tropics for the CCM3NOZM experiment, with little change poleward of 50° lat. Examination of the net radiation budget (a more reliable observational quantity) shows that the CRF change does represent a significant degradation of the CCM3NOZM TOA simulation between 15°N and 5°S, with a slight improvement in the subtropics, and relatively minor changes elsewhere. As before, we can crudely assess the role of the ''indirect'' effects of the deep convection scheme to the change in TOA radiative properties by adjusting the CCM3NOZM ocean energy transport requirements with the more realistic CCM3 TOA net radiation distribution. The modified ocean transport curve (''CCM3-adjusted'' CCM3NOZM) is shown in Fig. 3. Once again, this result suggests that although the degradation of the TOA energy distribution in the CCM3NOZM simulation represents a significant component of the change in the meridional ocean energy transport, it does not play the dominant role.

3. Surface energy budget analysis

As discussed earlier, the implied ocean meridional energy transport can be directly evaluated from the net surface energy budget. The results from the previous section demonstrate that TOA energy budget adjustments to this surface energy transport appear to play only a secondary role in the differences seen between the CCM2 and CCM3. Similarly, the TOA energy distribution changes associated with the ZM deep cumulus convection scheme also appear to play a secondary role in the implied meridional ocean energy transport changes. This indicates that there must be large modifications to the surface energy budget that are only weakly represented in the energy budget at the top of the atmosphere.

A direct examination of the surface energy budget components reveals marked differences between CCM2 and CCM3 in three of the four component fluxes. The major changes include a sharp reduction in absorbed solar flux in the mid- to high latitudes with a modest increase in the equatorial region, large systematic reductions in latent heat flux, particularly in the deep Tropics, and a systematic increase in the sensible heat flux. The question is whether the changes in any one of these components uniquely determine the improved meridional energy transport, or whether they are comparably responsible for the observed differences in T_O. A comparison of the CCM3 and CCM3NOZM surface energy

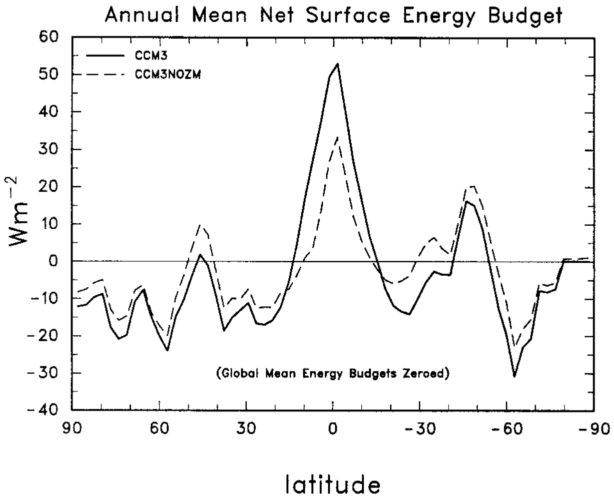

FIG. 4. Annual mean net surface energy budget for the CCM3 and CCM3NOZM experiment.

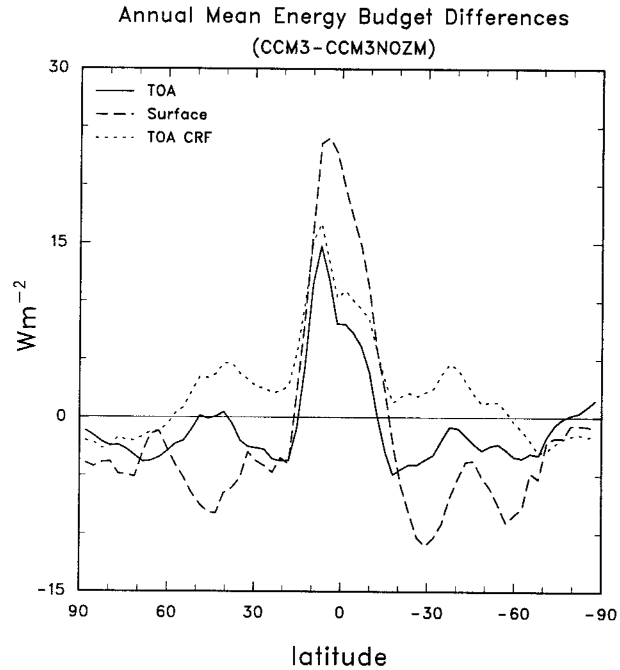

FIG. 5. Difference in the annual mean net surface and TOA energy budgets between the CCM3 and CCM3NOZM experiment. The corresponding difference in TOA net CRF is also included for reference.

budget components clearly answers this question, where the change in equatorial surface latent heat flux dominates the difference in the net surface energy budget. The absorbed solar energy, net longwave energy, and sensible heat flux all exhibit relatively minor differences, with maximum local changes of less than 5 W m^{-2}. The latent heat flux distribution exhibits comparably small changes throughout most of the domain except over the deep Tropics (10°N–10°S) where the latent heat flux in CCM3 is locally reduced by more than 20 W m^{-2} when compared to the simulation excluding the ZM deep convection scheme. The principal reason for this large reduction in LH is a systematic weakening of the surface winds in the deep Tropics (e.g., Collins et al. 1997).

The net surface energy budgets for the CCM3 and CCM3NOZM simulations are shown in Fig. 4. The change in equatorial latent heat flux associated with the incorporation of the deep convection scheme leads to an additional 24 W m^{-2} energy surplus just north of the equator. Outside the equatorial region, the introduction of the ZM deep convection scheme leads to a systematic reduction in the net surface energy balance with typical reductions of between 5 W m^{-2} and 10 W m^{-2}. As a result, the energy gradient between the equator and 30°S is enhanced by approximately 35 W m^{-2}. This enhanced pole to equator gradient in the net surface energy balance acts to increase the poleward energy transport required by the oceans in both the Northern and Southern Hemisphere. Physically, this enhanced gradient is dominated by a reduced cooling of the surface by latent energy fluxes in the deep Tropics and a weak increase of the sensible heat flux and net longwave radiation flux in the subtropics. The increased net longwave radiation in the subtropics appears to be in response to a slightly drier simulated atmosphere, another attribute of the deep convection scheme.

A comparison of the surface and TOA energy budget *differences* between the CCM3 and CCM3NOZM shows a similar meridional structure, where the CCM3 exhibits an additional equatorial energy surplus and stronger extratropical energy deficits in both curves (Fig. 5). The meridional gradients are considerably weaker at the TOA, however, where surface features like the extratropical minima are not reflected at the TOA. The net cloud radiative forcing differences (dotted line) show even weaker meridional gradients because of non-negligible changes in the clear-sky component of the cloud forcing. Thus, CRF differences only weakly reflect the changes in the net surface energy budget responsible for the rather dramatic differences in the implied meridional ocean energy transport between the CCM3 and CCM3NOZM simulations. This clearly explains why the CCM2 and CCM3NOZM meridional ocean energy transport curves are only moderately sensitive to the CCM3 TOA energy distribution adjustments applied in section 2.

4. Links between the TOA and surface energy budgets

As shown in section 2, changes in the TOA radiative energy budget do appear to be related to differences in the implied meridional ocean energy transport. Figure 5 also shows that the latitudinal distribution of the differences in TOA and surface net energy budgets bear some resemblence to each other, although for the simulations we have examined the TOA differences are of smaller amplitude than the more important differences at the surface. Differences in the TOA CRF are even weaker. Nonetheless, the similarity in the surface and TOA response raises a question about linkages between the energy budget signals seen at both the TOA and surface.

One strikingly different feature of the CCM3 simulation when compared to either the CCM2 or CCM3NOZM simulations is that upper-level equatorial cloud amount is significantly larger in the CCM3, by as much as 25% in the zonal annual mean. This feature of the CCM3 cloud distribution is what produces the large difference in the tropical net cloud radiative forcing, such as what is seen when comparing CCM2 and CCM3 in Fig. 2. A highly idealized experiment (NOZMCLD) was conducted to investigate the role of the increased high cloud amount on the surface energy budget and the implied meridional ocean energy transport. This experiment makes use of the CCM3NOZM model configuration, but includes a time invariant, zonally symmetric perturbation to the diagnosed cloud amount, A'_c, of the form:

$$A'_c = C \exp\left(\frac{-(|\phi - \phi_0|)}{\phi_h}\right) \times \begin{cases} [(p_0 - p)/\delta p - 1]^2[2(p_0 - p)/\delta p + 1] & p_0 - \delta p \le p < p_0 \\ [(p - p_0)/\delta p - 1]^2[2(p - p_0)/\delta p + 1] & p_0 + \delta p \ge p > p_0 \\ 0 \text{ elsewhere}, \end{cases} \quad (3)$$

where $C = 0.30$, $\delta p = 150$ mb, $\phi_0 = 5°$N, $\phi_h = 20°$ of latitude, and p_0 (in mb) is given by

$$p_0 = 500 - 250 \cos^2\phi. \quad (4)$$

This analytic function closely approximates the difference in zonally and annually averaged cloud amount between the CCM3 and CCM3NOZM simulations. In practice, the perturbation, A'_c, is not allowed to raise the total cloud fraction beyond 100%. Given the artificial way in which the cloud field is enhanced, this sensitivity experiment essentially explores the impact of an upper-level radiative forcing anomaly on the rest of the system. The NOZMCLD model configuration was integrated for 16 months using prescribed seasonally varying climatological SSTs, where the last 12 months (January–December) of the integration were used for the following analysis.

The properties of the NOZMCLD simulation are quite different from the CCM3NOZM experiment and much more like the CCM3 simulation. Many features in the CCM3 simulation are captured, such as a systematic warming of the upper-tropical troposphere. Examination of the longwave and shortwave radiative heating rate differences between CCM3 and CCM3NOZM (as well as NOZMCLD and CCM3NOZM) indicates that the

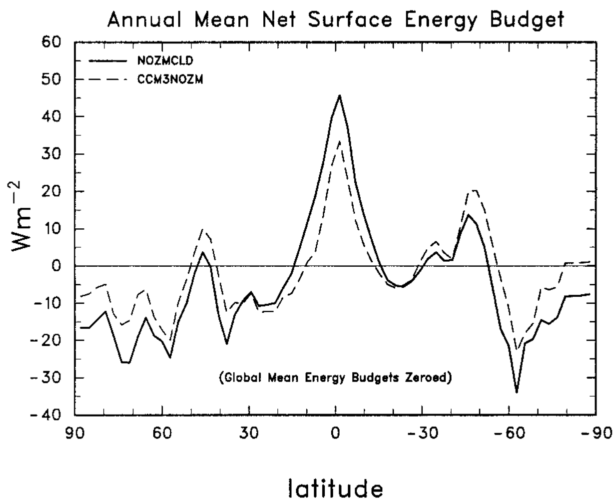

FIG. 6. Annual mean net surface energy budget for the NOZMCLD and CCM3NOZM experiments.

longwave heating response dominates the change in total diabatic heating by radiation. Even though the net radiative heating response is primarily in the longwave, the TOA and surface changes to the shortwave energy budget cannot be neglected. For example, the globally and annually averaged TOA and surface energy budgets are moderately imbalanced for this experiment, requiring a global energy correction of +6.57 W m^{-2} to the integrands in (1) and (2).

The corrected NOZMCLD and CCM3 *net* TOA energy budgets are reasonably similar to each other, although the longwave and shortwave energy component fluxes show non-negligible differences. The net surface energy budget changes also show a similar meridional structure when compared to the CCM3 simulation, with a broad increase in the tropical energy surplus and a systematic reduction elsewhere (Fig. 6). There are, however, significant differences in the amplitude of the response arising from some large differences in the individual component fluxes. The NOZMCLD surface latent heat flux shows a significant reduction in the equatorial region when compared to the CCM3NOZM simulation. The magnitude and structure of this reduction is comparable to what is produced by the CCM3 simulation. In this case, the latent heat flux reduction is in response to the combination of a slightly moister atmosphere and slightly weaker surface winds in the vicinity of the high cloud anomaly. Absorbed solar radiation in the equatorial region is substantially reduced, as are the net longwave and sensible heat fluxes (to a lessor extent). This response is quite different from the changes seen in the CCM3 simulation (compared to CCM3NOZM), where S_{sfc}, L_{sfc}, and SH all exhibit minor increases in the deep Tropics.

Latitudinal integration of the NOZMCLD net energy distribution yields an enhanced poleward energy transport requirement for the ocean in both hemispheres,

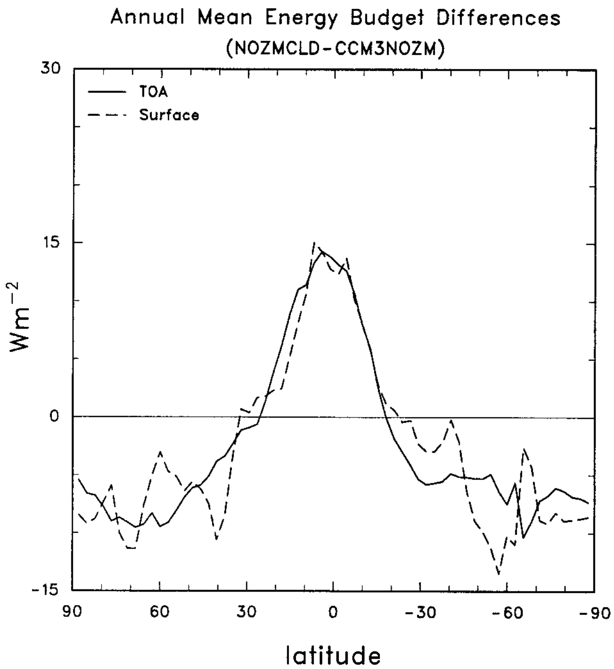

FIG. 7. Difference in the annual mean net surface and TOA energy budgets between the NOZMCLD and CCM3NOZM experiments.

similar to, but weaker than what is produced by the CCM3. More importantly, the differences in the net TOA and net surface energy budgets between the NOZMCLD and CCM3NOZM experiments show a remarkably close relationship between the TOA and surface (Fig. 7), in sharp contrast to the CCM3 and CCM3NOZM solutions (Fig. 5). These results suggest that a TOA radiative perturbation imposed on the climate system will be strongly reflected at the surface. Conversely, the earlier results from CCM3 and CCM3NOZM suggest that similarly large changes in the surface energy budget need not be reflected at the TOA.

Thus, the indirect effects of the deep convection parameterization in CCM3 (i.e., through the enhancement of high cloud amount) appear to introduce an anomaly of comparable magnitude in both the TOA and surface energy budgets. This anomaly does serve to improve the implied meridional ocean energy transport, as suggested by Gleckler et al. (1995). However, these results demonstrate that the CCM3's enhanced surface energy anomaly, seen in Fig. 5, cannot be traced to the indirect effects associated with increased high cloud amount, and must be attributable to a more direct effect of the deep convection parameterization on the surface energy budget (e.g., the incorporation of an abstraction for moist downdrafts).

5. Concluding remarks

The implied meridional ocean energy transport diagnosed from uncoupled integrations of the CCM3 represents a substantial simulation improvement when compared to the CCM2. The CCM3 simulation exhibits poleward energy transport requirements by the oceans with a magnitude and structure that very closely approximates observational estimates. Analysis of the changes in the simulated TOA energy budget suggests that the marked improvement in the CCM3 radiative energy distribution does not adequately explain the observed differences in meridional energy transport requirements at the surface. A systematic evaluation of the major updates to the CCM2 physical parameterizations reveals that the largest changes to the implied ocean energy transport accompany the introduction of the Zhang and McFarlane (1995) scheme for representing deep cumulus convection. The incorporation of this physical parameterization leads to a large decrease in equatorial latent heat fluxes. A reduced cooling of the surface by latent energy produces an additional energy surplus in the equatorial region and the need for enhanced poleward energy transport by the oceans. The most significant attribute of this change to the net surface energy budget is that it is only weakly reflected in the energy budget at the top of the atmosphere. Thus, the parameterization of moist convection, not the improved TOA simulation, appears to be playing the more important role in the determination of the more realistic surface energy budget in CCM3.

A numerical experiment to evaluate physical links between the TOA and surface energy budgets demonstrates that the radiative effects of high clouds strongly tie the two net energy budgets together. The imposition of a high cloud anomaly in a configuration of the CCM3 without the Zhang and McFarlane (1995) deep convection scheme produces a CCM3-like net radiative response at the top of the atmosphere, and an improvement in the meridional ocean energy transport characteristics. In this case, however, the changes to the TOA and surface net energy budgets are almost identical. This experiment suggests that anomalies in the TOA radiative energy budget are strongly reflected in the surface energy budget. The internal model physics parameterizations appear to do little to alter the magnitude or structure of the imposed TOA forcing as far as the net surface energy budget is concerned, even though there is a large latent heat flux response. This confirms the importance of properly simulating the TOA energy budget as argued by Gleckler et al. (1995). It also reemphasizes that something other than changes to the TOA radiation budget is playing the primary role in determining the CCM3 net surface energy budget, in this case, the particular formulation for parameterized cumulus convection.

The CCM's sensitivity to internal physical parameterization changes clearly demonstrates that the quality of the simulated TOA energy balance is but one measure of the quality of the simulated surface energy budget. The analysis results suggest that although the proper simulation of the TOA energy distribution is likely to be a necessary condition for the realistic representation of meridional surface energy transport, it is not sufficient. The meridional transport of energy from pole to equator at the surface cannot be uniquely characterized by any single measure of the simulation, but is ultimately determined by a complex nonlinear interaction of the collection of parameterized physical processes internal to the atmospheric model.

Acknowledgments. The author would like to acknowledge discussions of this topic with Jeffrey Kiehl and Byron Boville. I am also grateful to David Williamson for comments on an early version of the manuscript. Finally, my sincere thanks to David Randall for his support of a collaborative leave at Colorado State University, during which this work was completed.

REFERENCES

Barkstrom, B., H. Harrison, and R. Lee, 1990: The Earth Radiation Budget Experiment. *Eos, Trans. Amer. Geophys. Union,* **71,** 297–312.

Boville, B. A., and P. R. Gent, 1998: The NCAR Climate System Model, version one. *J. Climate,* **11,** 1115–1130.

Carissimo, B. C., A. H. Oort, and T. H. Vonder Haar, 1985: Estimating the meridional energy transports in the atmosphere and ocean. *J. Phys. Oceanogr.,* **15,** 82–91.

Collins, W. D., J. Wang, J. T. Kiehl, G. J. Zhang, D. I. Cooper, and W. E. Eichinger, 1997: Comparison of tropical ocean–atmosphere fluxes with the NCAR Community Climate Model, CCM3. *J. Climate,* **10,** 3047–3058.

Covey, C., 1988: Atmospheric and oceanic heat transport: Simulations versus observations. *Climate Change,* **13,** 149–159.

Gleckler, P. J., and B. C. Weare, 1997: Uncertainties in global ocean surface heat flux climatologies derived from ship observations. *J. Climate,* **10,** 2764–2781.

——, and Coauthors, 1995: Cloud-radiative effects on implied oceanic energy transports as simulated by atmospheric general circulation models. *Geophys. Res. Lett.,* **22,** 791–794.

Hack, J. J., 1994: Parameterization of moist convection in the National Center for Atmospheric Research Community Climate Model (CCM2). *J. Geophys. Res.,* **99,** 5551–5568.

——, 1998: Sensitivity of the simulated climate to a diagnostic formulation for cloud liquid water. *J. Climate,* in press.

——, B. A. Boville, B. P. Briegleb, J. T. Kiehl, P. J. Rasch, and D. L. Williamson, 1993: Description of the NCAR Community Climate Model (CCM2). NCAR Tech. Note NCAR/TN-382+STR, 108 pp. [NTIS PB93-221802/AS]

——, ——, J. T. Kiehl, P. J. Rasch, and D. L. Williamson, 1994: Climate statistics from the NCAR Community Climate Model (CCM2). *J. Geophys. Res.,* **99,** 20 785–20 813.

Hurrell, J. W., J. J. Hack, and D. P. Baumhefner, 1993: Comparison of NCAR Community Model climates. NCAR Tech. Note NCAR/TN-395+STR, 335 pp. [Available from NCAR, Boulder, CO 80307.]

Kiehl, J. T., J. J. Hack, and B. P. Briegleb, 1994: The simulated earth radiation budget of the NCAR CCM2 and comparisons with the Earth Radiation Budget Experiment (ERBE). *J. Geophys. Res.,* **99,** 20 815–20 827.

——, ——, G. B. Bonan, B. A. Boville, B. P. Briegleb, D. L. Williamson, and P. J. Rasch, 1996: Description of the NCAR Community Climate Model (CCM3). NCAR Tech. Note, NCAR/TN420+STR, 152 pp. [Available from NCAR, Boulder, CO 80307.]

——, ——, and J. W. Hurrell, 1998a: The energy budget of the NCAR Community Climate Model: CCM3. *J. Climate,* **11,** 1151–1178.

——, ——, G. B. Bonan, B. A. Boville, D. L. Williamson, and P. J. Rasch, 1998b: The National Center for Atmospheric Research Community Climate Model: CCM3. *J. Climate,* **11,** 1131–1149.

Kieth, D. W., 1995: Meridional energy transport: Uncertainty in zonal means. *Tellus,* **47A,** 30–44.

Oort, A. H., 1983: Global atmospheric circulation statistics, 1958–1973. NOAA Prof. Paper No. 14, National Oceanic and Atmospheric Administration, 180 pp.

Ramanathan, V., R. D. Cess, E. F. Harrison, P. Minnis, B. R. Barkstrom, E. Ahmad, and D. Hartmann, 1989: Cloud-radiative forcing and climate: Results from the Earth Radiation Budget Experiment. *Science,* **243,** 57–63.

Savijärivi, H. I., 1988: Global energy and moisture budgets from rawinsonde data. *Mon. Wea. Rev.,* **116,** 417–430.

Stone, P. H., and J. S. Risbey, 1990: On the limitations of general circulation climate models. *Geophys. Res. Lett.,* **17,** 2173–2176.

Trenberth, K. E., 1997: The heat budget of the atmosphere and ocean. *Proc. First Int. Conf. on Reanalysis,* Silver Spring, MD, 27–31.

——, and A. Solomon, 1994: The global heat balance: Heat transports in the atmosphere and ocean. *Climate Dyn.,* **10,** 107–134.

Zhang, G. J., and N. A. McFarlane, 1995: Sensitivity of climate simulations to the parameterization of cumulus convection in the Canadian Climate Centre general circulation model. *Atmos.–Ocean,* **33,** 407–446.